Journal of Bone Oncology 16 (2019) 100232

Contents lists available at ScienceDirect

Journal of Bone Oncology

journal homepage: www.elsevier.com/locate/jbo

Research Paper

Dovitinib dilactic acid reduces tumor growth and tumor-induced bone changes in an experimental breast cancer bone growth model

Tiina E. Kähkönen[a,b,*], Johanna M. Tuomela[a], Tove J. Grönroos[c,d,e], Jussi M. Halleen[b], Kaisa K. Ivaska[a], Pirkko L. Härkönen[a]

[a] University of Turku, Kiinamyllynkatu 10, 20520 Turku, Finland
[b] Pharmatest Services, Itäinen Pitkäkatu 4C, 5th floor, 20520 Turku, Finland
[c] Turku PET Centre, University of Turku, Tykistökatu 6A, 20520 Turku, Finland
[d] Medicity Research Laboratory, University of Turku, Turku, Finland
[e] Department of Oncology and Radiotherapy, Turku University Hospital, Turku, Finland

ARTICLE INFO

Keywords:
Breast cancer
Bone metastasis
Fibroblast growth factor receptor
Fibroblast growth factor receptor inhibitor
Dovitinib
TKI258

ABSTRACT

Advanced breast cancer has a high incidence of bone metastases. In bone, breast cancer cells induce osteolytic or mixed bone lesions by inducing an imbalance in bone formation and resorption. Activated fibroblast growth factor receptors (FGFRs) are important in regulation of tumor growth and bone remodeling. In this study we used FGFR1 and FGFR2 gene amplifications containing human MFM223 breast cancer cells in an experimental xenograft model of breast cancer bone growth using intratibial inoculation technique. This model mimics bone metastases in breast cancer patients. The effects of an FGFR inhibitor, dovitinib dilactic acid (TKI258) on tumor growth and tumor-induced bone changes were evaluated. Cancer-induced bone lesions were smaller in dovitinib-treated mice as evaluated by X-ray imaging. Peripheral quantitative computed tomography imaging showed higher total and cortical bone mineral content and cortical bone mineral density in dovitinib-treated mice, suggesting better preserved bone mass. CatWalk gait analysis indicated that dovitinib-treated mice experienced less cancer-induced bone pain in the tumor-bearing leg. A trend towards decreased tumor growth and metabolic activity was observed in dovitinib-treated mice quantified by positron emission tomography imaging with 2-[^{18}F]fluoro-2-deoxy-D-glucose at the endpoint. We conclude that dovitinib treatment decreased tumor burden, cancer-induced changes in bone, and bone pain. The results suggest that targeting FGFRs could be beneficial in breast cancer patients with bone metastases.

1. Introduction

In breast cancer, genetic alterations such as mutations, amplifications and gene fusions have been observed in fibroblast growth factor receptors (FGFRs) [1,2]. These alterations have been linked to poor prognosis, survival, and resistance to therapies in patients [1,2]. In breast cancer, most common and most extensively studied genetic alterations are in FGFR1 and FGFR2 genes [2,3]. Amplifications in FGFR1 are found in 10–15% of breast cancer patients having estrogen receptor negative (ER-) or human epidermal growth factor receptor 2 positive (HER2+) tumors [2–5]. Amplifications and mutations in FGFR2 are found particularly in triple-negative breast cancer (TNBC: ER-, progesterone receptor; PR- and HER2-), which is an aggressive subtype of breast cancer with limited treatment options [2,3]. For these reasons, FGFRs have become an attractive therapeutic target and currently there are several compounds under clinical investigations [1,3]. FGFR-targeting multikinase inhibitors have already been approved for other indications such as chronic myelogenous leukemia, gastrointestinal stromal tumors, advanced renal cell carcinoma and thyroid cancer, but so far not for breast cancer [1].

FGF family consists of 18 FGF-ligands that can activate FGFRs [6]. Of these, FGF1 and FGF2 (also known as basic FGF, bFGF) can activate all FGFRs, but the other FGFs only activate some of the receptors in a ligand and receptor specific manner [6]. FGFs signal from stroma to mesenchyme or *vice versa*, and can activate the receptors on the neighboring cells [6]. They act mainly in a paracrine manner in tissues, are important in embryogenesis, and are later involved in the development of diseases such as cancer [6]. There are four classical FGFRs

* Corresponding author at: Pharmatest Services, Itäinen Pitkäkatu 4C, 5th floor, 20520 Turku, Finland.
E-mail addresses: tiina.kahkonen@pharmatest.com (T.E. Kähkönen), jomitu@utu.fi (J.M. Tuomela), tovgro@utu.fi (T.J. Grönroos), jussi.halleen@pharmatest.com (J.M. Halleen), kakaiv@utu.fi (K.K. Ivaska), harkonen@utu.fi (P.L. Härkönen).

https://doi.org/10.1016/j.jbo.2019.100232
Received 8 January 2019; Received in revised form 17 March 2019; Accepted 18 March 2019
Available online 19 March 2019

named FGFR1-4, and an additional fifth receptor, FGFR-like 1 (FGFRL1 or FGFR5) [1]. FGFRs are receptor tyrosine kinases that are dimerized and activated upon FGF-ligand binding [1,3,6]. FGFRL1 is different from the other four receptors as it lacks the intracellular tyrosine kinase domain, and its functions are still unclear [1]. Once activated, FGFRs regulate many important pathways related to cancer growth and progression such as ERK-MAPK, PI3K-AKT and PLCy. They also activate pathways important for the maintenance of bone homeostasis such as the Wnt, the transforming growth factor beta (TGFβ), the hedgehog, and the bone morphogenic protein (BMP) pathways [1,3].

Molecular studies have shown that the FGF/FGFR pathways are important for cancer pathogenesis and progression as they regulate proliferation, migration and survival in various cell types [1,4,7,8]. FGFR1 has been linked to epithelial to mesenchymal transition (EMT), demonstrating a role in early metastatic process [5]. Additionally, FGFR1 has been shown to be important in interactions between malignant tumor and bone stromal cells in prostate cancer [8].The expression of FGFR1 and its ligands, FGF1 and FGF2 in particular, were shown to be elevated causing a paracrine activation of the pathway, resulting in the formation of osteolytic bone lesions *in vivo* [8,9]. Additionally, we have previously demonstrated the effects of FGF8 on formation of osteolytic bone lesions [9]. In bone, the FGF/FGFR pathways are important in the maintenance of bone homeostasis by bone resorption and formation [10–12]. FGFR1 is important for the differentiation and function of bone-resorbing osteoclasts [10], and FGFR1 deficiency reduces the number and activity of osteoclasts in mice [11]. In contrast, FGFR2 is important for the differentiation and function of osteoblasts [11–13]. FGFR2 knockout mice have defects in bone formation due to a malfunction of osteoblasts [10]. FGFs can also promote or inhibit osteoclast and osteoblast function and activity by different mechanisms [10]. Only a few studies have evaluated the effects of FGFR inhibitors on bone. Lee et al. showed that dovitinib enhances osteoblast differentiation *in vitro* by increasing the expression of osteoblast target genes [14]. The results by Aukes et al. suggest that FGFR inhibitor BGJ398 alone has no effect on resorption activity of osteoclasts *in vivo* [10].

Some studies have evaluated the effects of FGFR inhibitors on lung metastases with promising results [5,15,16], but only a few studies have been published on the effects of FGFR inhibitors in the context of bone metastasis. The study by Aukes et al. demonstrates that tumor cells increase osteoclast differentiation and activity *in vivo,* and in a co-culture setting of osteoclasts and breast cancer cells, BGJ398 reduces the activation of FGFR-mediated signaling and decreases the expression of osteoclast target genes [10]. These findings warrant for further studies to understand the communication of tumor and bone cells at metastatic sites.

Dovitinib dilactic acid (TKI258) is a non-selective FGFR inhibitor, which blocks not only FGFR1, FGFR2, and FGFR3, but also other tyrosine kinase receptors such as c-Kit and vascular endothelial growth factor receptors (VEGFRs) [8,14,16,17]. We have previously demonstrated that 1 μM TKI258 inhibits proliferation of MFM223 breast cancer cells *in vitro* (Kähkönen et al., unpublished observation). Others have also reported that TKI258 is potent in decreasing proliferation and migration of mouse breast cancer cells [16]. Treatment of tumor-bearing mice with dovitinib reduces tumor growth by impairing cell survival and decreasing vascular density [16,17]. Furthermore, dovitinib impairs the formation of lung metastases [16]. In a patient-derived xenograft (PDX) model of prostate cancer bone metastasis, dovitinib had anti-tumor activity, which was concluded to be partially due to modulation of bone microenvironment [8]. Dovitinib is currently in phase I/II/III clinical trials for the treatment of several cancer types with genetic alterations in FGFRs, including advanced breast cancer [14].

Bone is the most preferred site for metastasis in breast cancer. Because inhibition of FGFRs has shown promising potency in decreasing tumor growth and maintaining bone homeostasis, we aimed to evaluate the effects of dovitinib on growth of FGFR1 and FGFR2 amplified MFM223 breast cancer cells *in vivo* using an intratibial bone growth model.

2. Methods

2.1. Cell culture and dovitinib

MFM223 human breast cancer cells (Sigma Aldrich) were cultured in DMEM (Sigma Aldrich) with 10% inactivated fetal bovine serum (Gibco) and penicillin-streptomycin (Gibco) in humidified incubator (37 °C, 5% CO_2). For animal experiments, 500,000 cells were suspended in 20 μl of phosphate buffered saline (Gibco). Cell viability was determined with automated cell counter (Bio-Rad) using trypan blue (Bio-Rad) as a marker for dead cells before inoculation of the cancer cells, and after inoculation from the remaining cell stock. The cell viability was above 90% after the inoculation.

Dovitinib dilactic acid (TKI258) was purchased from Selleck Chemicals. It was diluted in sterile water, filtered with 0.2 μm filter and stored at −20 °C in aliquots until used as instructed by the manufacturer.

2.2. Intratibial mouse model and animal experiment license

Animal experiments were carried out in the Central Animal Facility, University of Turku, with an animal experiment license granted by the National Animal Experimental Board of Southwest Finland (ESAVI2329/04.10.07/2017).

Five to six weeks old immunocompromised Balb/c-nude mice (Janvier) were used ($n = 19$ in the first study and $n = 20$ in the second study). Prior to intratibial injection the mice were given an analgesic (Temgesic, buprenorphine, 0.3 mg/ml; Reckitt&Coleman). For the inoculation, the mice were placed under isoflurane anesthesia (ScanVet; induction 4% and maintenance 2%). To perform the inoculations, a 29G insulin needle (BD) was used to drill a hole through the growth plate in proximal tibia. The right position of the needle was ensured by X-ray imaging and a second needle was used to inoculate the cells through the hole to the bone marrow. On the following day, the mice were inspected and a second dose of Temgesic was administrated.

After 4 weeks, the mice were randomized in two groups ($n = 9$–10 in both groups). The mice received a daily 40 mg/kg p.o. dose of dovitinib by oral gavage (Instech) or an equal volume of vehicle (100 μl, sterile water) for 5 weeks. The dose was adopted from the study by Dey et al. [16].

At the end of the study, the mice were sacrificed by inhalation of CO_2 and the death was confirmed by cervical dislocation. Blood samples were collected by heart puncture, centrifuged (2000 × G, 30 min), and the serum was stored at −70 °C. The inoculated tibias were fixed in 10% neutral buffered formalin for 48 h and stored in 70% ethanol.

2.3. PET/CT imaging

Positron emission tomography (PET; Inveon PET/CT, Siemens Medical Solutions, Knoxville, TN) imaging using 2-[^{18}F]fluoro-2-deoxy-D-glucose ([^{18}F]FDG) was performed in five mice from both groups. The mice were placed under isoflurane anesthesia and 4.68 ± 1.06 MBq of [^{18}F]FDG was administered intravenously 120 min before the PET scan. In order to prevent uptake of the tracer into leg muscles, the mice were kept anesthetized during the 120 min waiting period. The mice were then placed in the central field of view of the scanner, and a low-resolution 10 min CT scan was launched and used for attenuation correction, followed by a 20 min static emission PET scan. During the scans, body temperature of the mice was kept at 37 °C with a heating pad on the scanner bed. The PET images were reconstructed using Fourier rebinning and a two-dimensional filtered back-projection algorithm. Reconstructed images were analyzed with Siemens Inveon

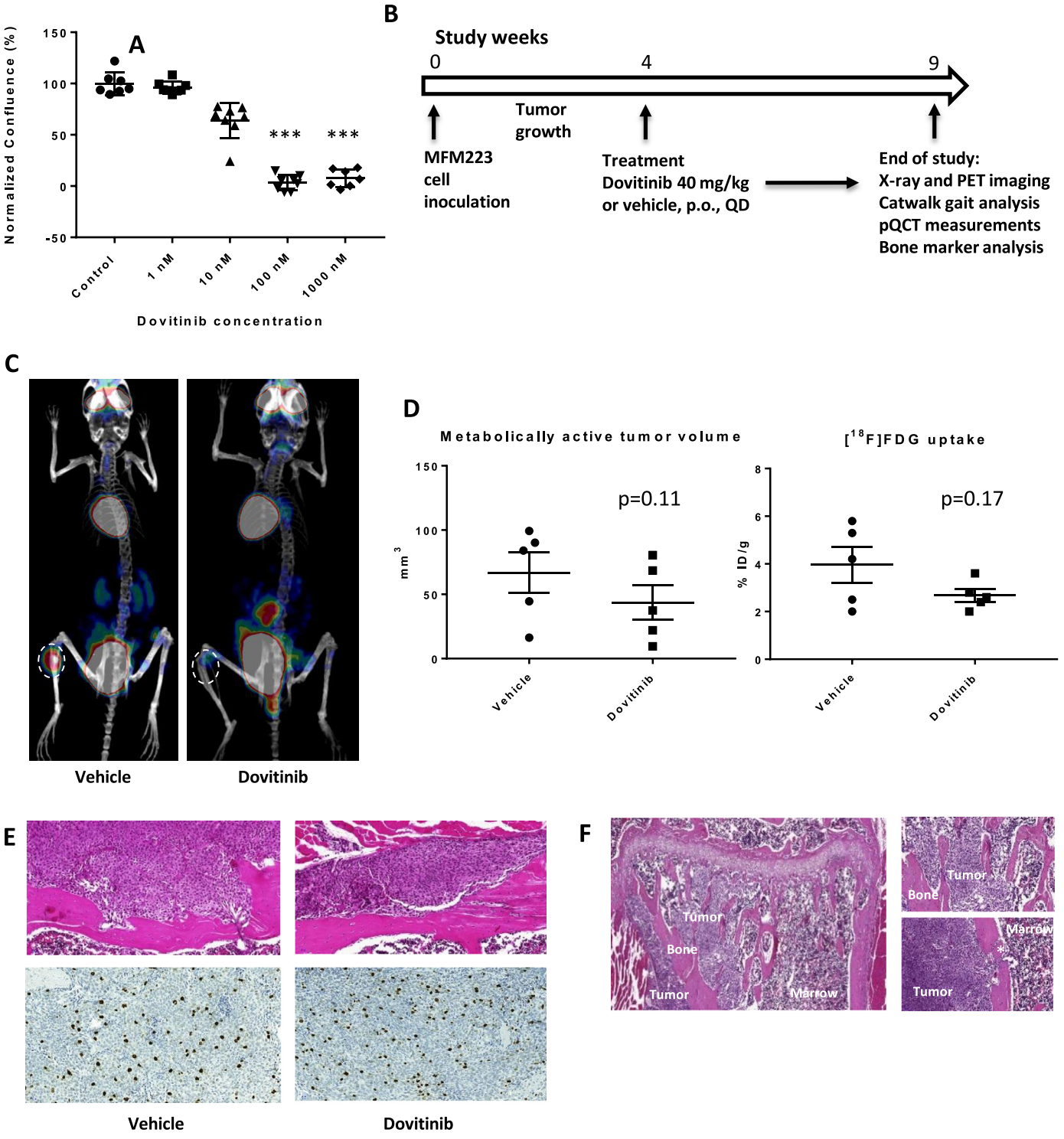

Fig. 1. (A) Proliferation of MFM223 cells *in vitro* measured as well confluency (%, mean ± SD) after 48 h incubation with different concentrations of dovitinib. (B) Timeline of the study. MFM223 breast cancer cells were inoculated into the proximal tibia at day 0. The tumors were allowed to grow for 4 weeks, after which the mice were treated with dovitinib (40 mg/kg, p.o.) or vehicle daily (QD) for 5 weeks. At endpoint, X-ray and PET imaging, CatWalk gait analysis, pQCT and serum TRACP5b measurements were performed. (C) Representative images from [^{18}F]FDG PET/CT imaging. Location of the tumor is marked with dotted lines. (D) The metabolically active tumor volume (mm^3) and [^{18}F]FDG uptake (% ID/g) analyzed from PET/CT images. Individual values are presented with dots and the horizontal line presents the group mean ± SEM, $n = 5$. The differences between treated and control groups did not reach statistical significance ($p > 0.05$). (E) Representative HE and PHH3 stainings of tumors from vehicle and dovitinib treated mice, 20× magnification. (F) HE stained tumor sections, magnification 6× and 20×, from one mouse. Tumor growth was observed inside the bone marrow cavity and also externally on periosteal surface. Tumor cells migrating out from the bone marrow cavity are marked with a white asterisk (*).

Research Workplace software (version 4.0, Siemens Preclinical Solutions) by manually placing regions of interest (ROIs) around the tumor. The uptake of [^{18}F]FDG into the tumor ROIs (indicating metabolic activity) was expressed as the percent of injected dose per gram tissue (% ID/g). The values were corrected for the injected activity and the injection time (decay). The size of the ROIs indicated

metabolic active tumor volume (mm^3).

2.4. Histology

Tumor-bearing tibias were decalcified in 10% EDTA for two weeks. EDTA solution (Sigma-Aldrich) was changed to fresh every 4–6 days. After decalcification, the samples were embedded in paraffin and cut longitudinally to 5 μm thin sections. The tibias were cut through, and the sections were stained from 5 different levels with hematoxylin-eosin (HE) to visualize tumor cells.

2.5. X-ray imaging and analysis

X-ray imaging (Faxitron MX-20; settings 37 kW for 7 s) was performed weekly to monitor the development of tumor-induced changes in bone (bone lesions). The area of bone lesions (pixels) was analyzed with ImageJ software from the endpoint X-ray images.

2.6. pQCT imaging and analysis

Peripheral quantitative computed tomography (pQCT, Norland Stratec) was used to image and analyze formalin-fixed tumor-bearing tibias *ex vivo*. For imaging, the bones were placed on plastic holder and pre-scanned to determine the correct analysis site. The scannings were performed at the area of trabecular bone 0.7–1 mm below the growth plate, and the area was separately defined for all samples. A voxel size of 70 μm and diameter of 10 mm were used in the scannings. Total, trabecular and cortical bone mineral content (BMC, mg/mm) and bone mineral density (BMD, mg/mm^3) were analyzed from each sample.

2.7. Serum TRACP5b measurements

Serum samples were analyzed for mouse tartrate resistant acid phosphatase 5b (TRACP5b; MouseTRAP, IDS) used as a marker for osteoclast number [18]. Five microliters of serum was used for the analysis and the assay was performed according to the instructions provided by the manufacturer. Absorbance was measured using a microplate reader (Victor2, PerkinElmer).

2.8. CatWalk analysis

Movement-related pain was monitored using CatWalkXT (Noldus) gait analysis at endpoint. The mice had a training period of 3 times to familiarize with the platform before the experiment was performed. The mice were placed on the CatWalkXT platform and allowed to walk freely on the runway for three replicate runs. The runs were analyzed for each mouse using CatWalkXT analysis software. Special attention was paid to effects on tumor-bearing legs of the mice.

Bone pain in the tumor-bearing leg (right hind paw) was analyzed by measuring the print area and maximum contact area (both cm^2). The movement was analyzed by measuring body speed and stands (both seconds), step cycle (s), stride length (cm) and swing speed (cm/s).

2.9. Statistical analysis

Statistical analysis was performed with GraphPad Prism 7 software using Mann–Whitney *U* test. Statistical significances are marked as NS = non-significant, $*p < 0.05$, $**p < 0.01$, and $***p < 0.001$.

Two independent experiments were performed. The total number of mice was 19 (vehicle group, $n = 10$ and dovitinib-group, $n = 9$) in the first experiment and 20 in the second experiment ($n = 10$ in both groups). The main findings were similar in both studies and the data from the second study is reported.

3. Results

3.1. Dovitinib-treatment was associated with decreased tumor growth

MFM223 cells were inoculated into tibia bone marrow of nude mice at day 0 (Fig. 1(A)). The tumors were allowed to grow for 4 weeks, after which the treatment was started and continued for 5 weeks (Fig. 1(A)). [^{18}F]FDG imaging was performed at the endpoint. Fig. 1(B) shows [^{18}F]FDG uptake in tumor, heart, kidneys and bladder. Statistically significant differences were not observed in [^{18}F]FDG uptake in tumor ($p = 0.17$, NS) and metabolic active tumor volume ($p = 0.11$, NS) in tumor-bearing tibia from dovitinib-treated mice compared to vehicle-treated mice (Fig. 1(C)). However, there was a trend of decrease in both parameters by dovitinib treatment, which was consistent with our other observations. Based on histology at the endpoint, the tumors were predominantly growing close to cortical bone surfaces and the tumor cells migrated to extraosseal space, disabling reliable quantitation of tumor area (Fig. 1(D)).

3.2. Dovitinib reduced cancer-induced bone changes

The development of tumor-induced bone lesions was followed by X-ray imaging (Fig. 2(A)). At the beginning of the treatment (4 weeks in study) 40–45% of the mice had prominent bone changes that later developed into bone lesions. At the endpoint (9 weeks in study) over 90% of the mice had bone lesions that were osteolytic-mixed in this model (Fig. 2(A)). The lesion area was quantified from the X-ray images at the endpoint, and the bone lesion area was smaller in dovitinib-treated mice compared to vehicle-treated mice ($p = 0.036$, Fig. 2(B)).

Dovitinib-treated mice had lower TRACP 5b serum levels compared to vehicle-treated mice ($p = 0.0019$ Fig. 2(C)), suggesting that dovitinib treatment decreased the number of osteoclasts. Changes in BMC and BMD were analyzed by pQCT *ex vivo* (Fig. 2(D)). Total BMC was higher in dovitinib-treated mice compared to vehicle-treated mice ($p = 0.0037$). This change was related to increased cortical BMC ($p = 0.0039$) and BMD ($p = 0.034$), while no changes were observed in trabecular bone.

3.3. Dovitinib treatment was associated with reduced bone pain

At endpoint, visual estimation suggested that mobility of the mice had changed. CatWalk gait analysis was performed to quantitate changes in how the mice moved and walked to estimate cancer-induced bone pain in the model. Observations from the CatWalk analysis were divided into two categories: changes in the pressure placed on the hind paw (Fig. 3(A)) and changes in mouse movement (Fig. 3(B)). Print area ($p = 0.027$) and maximum contact area ($p = 0.018$) were larger in dovitinib-treated mice compared to vehicle-treated mice. Dovitinib-treated mice moved faster compared to the vehicle-treated mice (body speed, $p = 0.0086$) and had less stands ($p = 0.0066$) probably due to increased body speed. The step cycle was decreased ($p = 0.019$), while the stride length and swing speed were increased ($p = 0.0072$ and $p = 0.014$, respectively).

4. Discussion

Treatment options for bone metastases are limited and new therapies are urgently needed. FGFR signaling is important both in cancer and bone, making targeting the pathway an interesting option when considering development of new treatments for bone metastatic disease. In this study, we evaluated the effects of dovitinib on FGFR-amplified breast cancer cells inoculated into bone as a model of bone metastasis. We used MFM223 human breast cancer cells that are reported to have amplifications in both FGFR1 and FGFR2 [19]. We have previously found that these cells are sensitive to dovitinib *in vitro* and *ex vivo* (Kähkönen et al., unpublished observations).

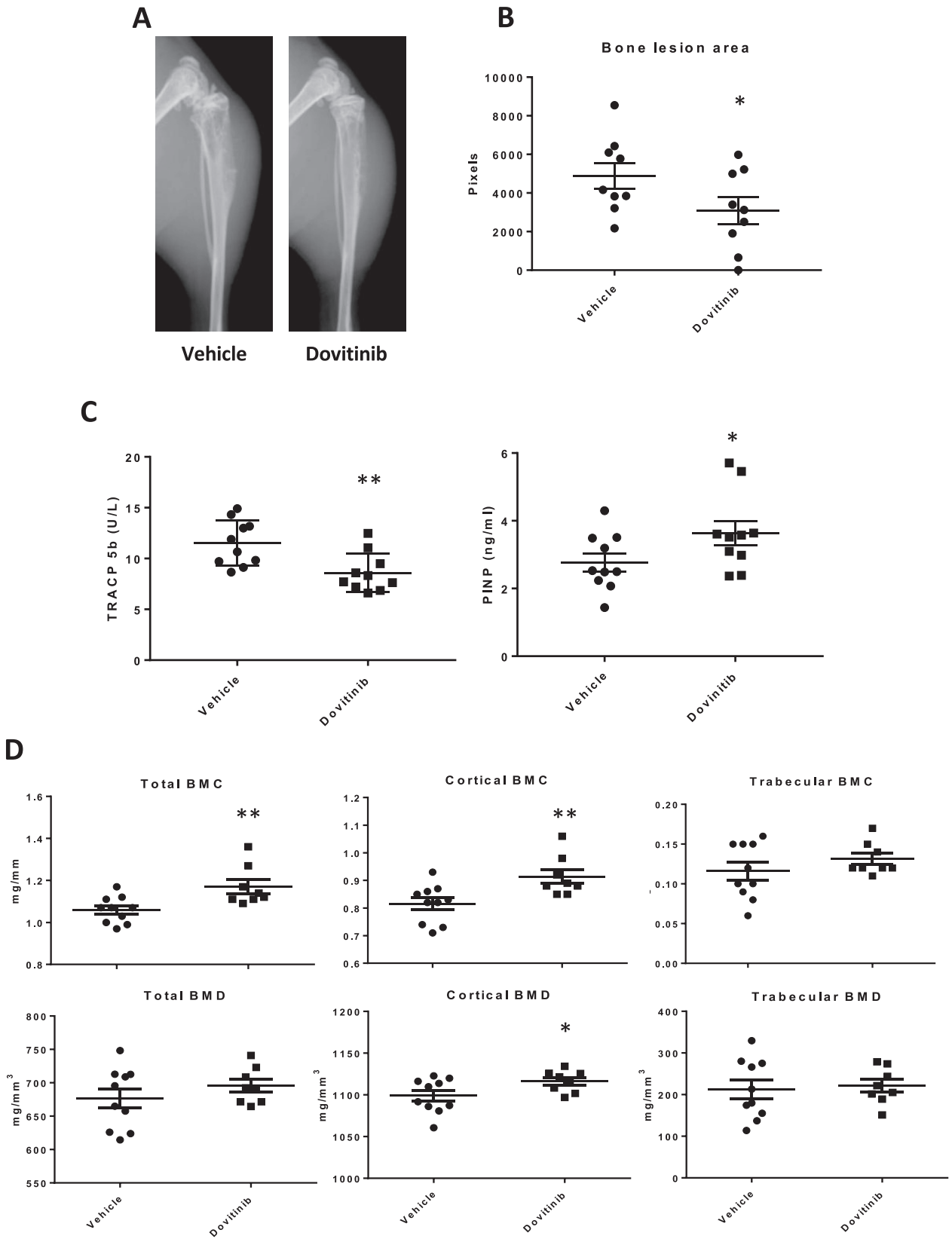

Fig. 2. (A) Representative X-ray images taken at the end point for vehicle- and dovitinib-treated mice. (B) The X-ray images were analyzed for the area of bone changes (bone lesions). Individual values are presented as dots and the means ± SEM are shown by horizontal lines. (C) TRACP5b and PINP levels were measured from serum samples and used as markers of number of osteoclasts and bone formation, respectively. Individual values are presented as dots and the means ± SEM as horizontal lines. (D) Bone mineral content (BMC) and density (BMD) were analyzed by pQCT. Total, cortical and trabecular BMC and BMD are reported from tumor-bearing tibia. Individual values are presented as dots with the mean ± SEM as horizontal lines. Statistically significant differences are marked as * $p < 0.05$, ** $p < 0.001$.

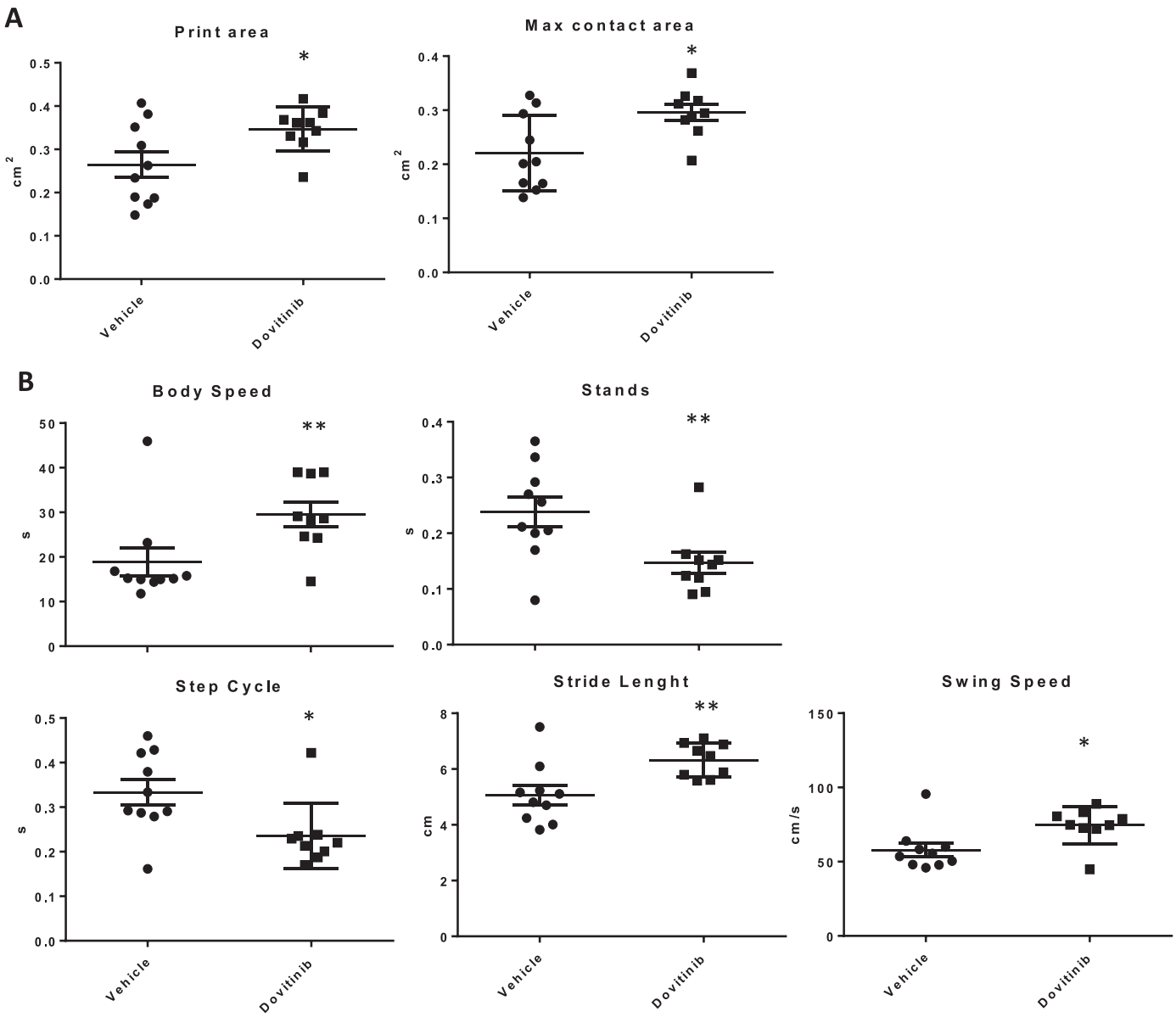

Fig. 3. (A) Cancer-induced bone pain was measured by CatWalk gait analysis. The print area (cm^2) and max contact area (cm^2) are reported for the tumor-bearing leg. (B) Mouse movement was monitored by recording body speed (s), stands (s), step cycle (s), stride length (cm) and swing speed (cm/s). Individual values are presented as dots and the mean ± SEM shown as horizontal lines. Statistically significant differences are marked as $*p < 0.05$, $**p < 0.001$.

The detection of tumors can be challenging in metastasis models with cells without fluorescent or luciferase labels. We and others have shown that tumors growing in the bone can be detected using [^{18}F]FDG [20] or other PET tracers [21]. Although the differences did not reach statistical significance, [^{18}F]FDG/PET imaging revealed a trend in decreased metabolic active tumor volume and metabolic activity ([^{18}F]FDG uptake) in treated animals. One of the limitations in this study was the low number of mice (n = 5/group) that could be used for PET imaging, which might have resulted in lack of statistical power. However, tumors treated with dovitinib were markedly smaller by visual estimation of the PET images.

Tumor-induced bone changes were monitored by X-ray imaging during the study. MFM223 cells induced bone changes that were predominantly osteolytic or mixed. This phenotype is also typical for breast cancer patients. The treatment with dovitinib was started when the tumors had grown in bone for 4 weeks, and thereafter the treatment was continued consecutively for 5 weeks. The used dose of dovitinib as monotherapy was not adequate to prevent the tumors from growing in bone. Therefore, combination treatments are warranted. In ongoing clinical trials, combinations of dovitinib with an aromatase inhibitor (NCT01484041), fulvestrant (NCT01528345) and paclitaxel (NCT01548924) have been investigated, but the studies have been interrupted and terminated for various reasons.

Potentially, dovitinib may have a dual effect on bone metastases, affecting both tumor growth and bones. This was suggested by Lee et al. who also showed that dovitinib increased the number of osteoblasts, resulting in increased bone formation [14]. A combination of anabolic bone effects with the anti-tumor properties of dovitinib shown here might further decrease the formation of osteolytic bone lesions. Agents with both anti-tumor and anabolic bone effects might be beneficial in the treatment of osteolytic bone metastases in patients.

Accompanied with a trend towards decreased tumor volume and a significant decrease in bone lesion area, we observed higher total BMC in dovitinib-treated mice compared to vehicle-treated mice. Histological analysis revealed that the tumor cells were growing predominantly in a close proximity to bone surfaces and preferably

migrated to grow outside of bone marrow cavity. This migration process has also been previously described [9]. The tumor growth predominantly on cortical bone surfaces may also explain the observed changes in cortical bone in this study, and they may also be partly caused by the anabolic bone effects discussed in the previous paragraph.

One limitation of the study was the lack of sham-operated control mice. The use of sham-operated mice would have allowed comparison of BMD to healthy mice. Similar findings were also reported by Aukes et al., who did not observe a decrease in tumor growth by bioluminescence imaging with the FGFR inhibitor BGJ398, but observed an increased bone volume in a model where breast cancer cells were injected into the femur [10]. They also showed that the treatment had no effect on sham-operated bones [10]. In our study, we observed lower serum TRACP5b levels in dovitinib-treated mice indicating that the systemic number of osteoclasts was decreased. This is controversial to the observation of Aukes et al. who showed that TRACP5b levels were increased, but also that the ratio of TRACP5b to CTX-I serum levels demonstrating the systemic "resorption index" was decreased [10]. However, this can be explained by the used different cell line and FGFR-inhibitor, and formation of larger osteolytic lesions compared to our model.

Patients with bone metastases often have serious bone pain, which has a great impact on their quality of life [10]. Therefore, we also monitored cancer-induced bone pain in the mice by CatWalk gait analysis. Our results indicate that bone pain was reduced by dovitinib treatment in the leg where the cancer cells had been inoculated.

To the best of our knowledge, this is the first study in which the effects of dovitinib on breast cancer have been evaluated in a bone metastatic setting. The effects of dovitinib have been previously studied in a subcutaneous breast cancer xenograft model *in vivo* with the HBCx-2 model that has 8 FGFR1 gene copies, and in the HBCx-3 model with 10 FGFR2 gene copies [22]. In the HBCx-2 model, a dose of 30 mg/kg and 50 mg/kg resulted in decreased tumor growth or tumor regression, respectively [22]. In the HBCx-3 model, a dose of 40 mg/kg caused tumor regression [22]. The effects of FGFR inhibitors on lung metastasis have also been evaluated. Issa et al. have shown that combinations of dovitinib with a PI3K/mTOR-inhibitor and with an ErbB2-inhibitor decreased breast cancer tumor growth in lungs [17]. Brown et al. have evaluated the effects of the FGFR inhibitor FIIN-4 on breast cancer lung metastasis *in vivo* [5], showing that FIIN-4 inhibited metastatic tumor growth. They also demonstrated that FGFR1 co-operated with β3 integrin and FAK in promoting EMT, providing a proof-of-concept that these routes are important in metastatic disease [5].

We conclude that treatment of nude mice bearing intratibial MFM223 breast cancer xenografts with the FGFR inhibitor dovitinib decreased tumor growth in bone and cancer-induced bone changes. Dovitinib treatment was also associated with a decrease in cancer-induced bone pain. However, despite the positive effects of treatment, the tumors continued to grow in mice, indicating a need for treatment combinations for better overall efficacy.

Acknowledgments

We would like to thank Ms Liudmila Shumskaya and Ms Soili Jussila for their technical assistance in processing the histological samples and performing the stainings.

Authors' contributions

Kähkönen TE: Planning and conducting the study, collection and analysis of the data, and responsible for writing the first draft of the manuscript. Tuomela JM: Planning and assisting with the execution of the study. Grönroos TJ: Planning and assisting with the PET study. Halleen JM: Supervising bone analysis. Ivaska KK and Härkönen PL: Planning and supervising the study. All authors have contributed to writing the manuscript and accepted it to be submitted for publication.

Availability of data and materials

The data will be available by contacting the corresponding author.

Financial support and sponsorship

Kähkönen TE: Drug Discovery Doctoral Programme of University of Turku. Härkönen PL: The Sigrid Jusélius Foundation and the Academy of Finland.

Conflicts of interest

Halleen JM: receipt of royalties from IDS Plc. Other authors declare no conflicts of interest.

Ethical approval and consent to participate

Not applicable.

Consent for publication

Not applicable.

Supplementary materials

Supplementary material associated with this article can be found, in the online version, at doi:10.1016/j.jbo.2019.100232.

References

[1] T. Helsten, M. Schwaederle, R. Kurzrock, Fibroblast growth factor receptor signaling in hereditary and neoplastic disease: biologic and clinical implications, Cancer Metastasis Rev. 34 (3) (2015) 479–496.
[2] I.S. Babina, N.C. Turner, Advances and challenges in targeting FGFR signalling in cancer, Nat. Rev. Cancer 17 (5) (2017) 318–332.
[3] A.E. Fearon, C.R. Gould, R.P. Grose, FGFR signalling in women's cancers, Int. J. Biochem. Cell Biol. 45 (12) (2013) 2832–2842.
[4] C.Y. Shiang, Y. Qi, B. Wang, V. Lazar, J. Wang, W. Fraser Symmans, et al., Amplification of fibroblast growth factor receptor-1 in breast cancer and the effects of brivanib alaninate, Breast Cancer Res. Treat. 123 (3) (2010) 747–755.
[5] W.S. Brown, L. Tan, A. Smith, N.S. Gray, M.K. Wendt, Covalent targeting of fibroblast growth factor receptor inhibits metastatic breast cancer, Mol. Cancer Ther. 15 (9) (2016) 2096–2106.
[6] A. Beenken, M. Mohammadi, The FGF family: biology, pathophysiology and therapy, Nat. Rev. Drug Discov. 8 (3) (2009) 235–253.
[7] M. Katoh, H. Nakagama, FGF receptors: cancer biology and therapeutics, Med. Res. Rev. 34 (2) (2014) 280–300.
[8] X. Wan, P.G. Corn, J. Yang, N. Palanisamy, M.W. Starbuck, E. Efstathiou, et al., Prostate cancer cell-stromal cell crosstalk via FGFR1 mediates antitumor activity of dovitinib in bone metastases, Sci. Transl. Med. 6 (252) (2014) 252ra122.
[9] M.P. Valta, J. Tuomela, A. Bjartell, E. Valve, H.K. Vaananen, P. Harkonen, FGF-8 is involved in bone metastasis of prostate cancer, Int. J. Cancer 123 (1) (2008) 22–31.
[10] K. Aukes, C. Forsman, N.J. Brady, K. Astleford, N. Blixt, D. Sachdev, et al., Breast cancer cell-derived fibroblast growth factors enhance osteoclast activity and contribute to the formation of metastatic lesions, PLoS One 12 (10) (2017) e0185736.
[11] D.M. Ornitz, P.J. Marie, Fibroblast growth factor signaling in skeletal development and disease, Genes Dev. 29 (14) (2015) 1463–1486.
[12] X. Du, Y. Xie, C.J. Xian, L. Chen, Role of FGFs/FGFRs in skeletal development and bone regeneration, J. Cell Physiol. 227 (12) (2012) 3731–3743.
[13] T.E. Kahkonen, K.K. Ivaska, M. Jiang, K.G. Buki, H.K. Vaananen, P.L. Harkonen, Role of fibroblast growth factor receptors (FGFR) and FGFR like-1 (FGFRL1) in mesenchymal stromal cell differentiation to osteoblasts and adipocytes, Mol. Cell Endocrinol. 461 (2018) 194–204.
[14] Y. Lee, K.J. Bae, H.J. Chon, S.H. Kim, S.A. Kim, J. Kim, A receptor tyrosine kinase inhibitor, dovitinib (TKI-258), enhances BMP-2-induced osteoblast differentiation in vitro, Mol. Cells 39 (5) (2016) 389–394.
[15] A. Sahores, M. May, G. Sequeira, C. Fuentes, B. Jacobsen, C. Lanari, et al., Targeting FGFR with BGJ398 in breast cancer: effect on tumor growth and metastasis, Curr. Cancer Drug Targets 18 (10) (2018) 979–987.
[16] J.H. Dey, F. Bianchi, J. Voshol, D. Bonenfant, E.J. Oakeley, N.E. Hynes, Targeting fibroblast growth factor receptors blocks PI3K/AKT signaling, induces apoptosis, and impairs mammary tumor outgrowth and metastasis, Cancer Res. 70 (10) (2010) 4151–4162.
[17] A. Issa, J.W. Gill, M.R. Heideman, O. Sahin, S. Wiemann, J.H. Dey, et al.,

Combinatorial targeting of FGF and ErbB receptors blocks growth and metastatic spread of breast cancer models, Breast Cancer Res. 15 (1) (2013) R8.
[18] S.L. Alatalo, J.M. Halleen, T.A. Hentunen, J. Monkkonen, H.K. Vaananen, Rapid screening method for osteoclast differentiation *in vitro* that measures tartrate-resistant acid phosphatase 5b activity secreted into the culture medium, Clin. Chem. 46 (11) (2000) 1751–1754.
[19] N. Turner, A. Pearson, R. Sharpe, M. Lambros, F. Geyer, M.A. Lopez-Garcia, et al., FGFR1 amplification drives endocrine therapy resistance and is a therapeutic target in breast cancer, Cancer Res. 70 (5) (2010) 2085–2094.
[20] W. Zhou, P. Xie, M. Pang, B. Yang, Y. Fang, T. Shu, et al., Upregulation of CRMP4, a new prostate cancer metastasis suppressor gene, inhibits tumor growth in a nude mouse intratibial injection model, Int. J. Oncol. 46 (1) (2015) 290–298.
[21] C.W. Huang, W.C. Hsieh, S.T. Hsu, Y.W. Lin, Y.H. Chung, W.C. Chang, et al., The use of PET imaging for prognostic integrin $\alpha_2\beta_1$ phenotyping to detect non-small cell lung cancer and monitor drug resistance responses, Theranostics 7 (16) (2017) 4013–4028.
[22] F. Andre, T. Bachelot, M. Campone, F. Dalenc, J.M. Perez-Garcia, S.A. Hurvitz, et al., Targeting FGFR with dovitinib (TKI258): preclinical and clinical data in breast cancer, Clin. Cancer Res. 19 (13) (2013) 3693–3702.